Indirect Robust Adaptive Nonlinear Controller Design for a New 3D Chaotic System

Olivier Baraka Mushage

Université Libre des Pays des Grands Lacs, Faculty of Applied Sciences and Technologies
olivermushage[at]gmail.com

Abstract:A ***new three-dimensional chaotic system is presented with its basic properties such as equilibrium points, Lyapunov's exponents and Kaplan-Yorke dimension. An Indirect Robust Adaptive Nonlinear Controller for complete synchronization and/or control of the new system considered with mismatch disturbancesis designed. The adaptive controller is designed such that it allows simultaneously accurate control and system identification. The same controller design approach proposed in this paper can be applied to the design of controllers for other nonlinear Multi-Input-Multi Output (MIMO) systems with parameters uncertainties. Using the Lyapunov's method, the update rules for system identification are derived. MATLAB simulations results are presented to illustrate the efficiency of the proposed controller.***

Keywords: Indirect adaptive controller; chaotic system; chaos control; chaos synchronization; system identification.

1. Introduction

Since its description for the first time in 1963 by the physicist E. Lorenz as a deterministic nonperiodic flow, continuous chaos has gain considerable attention in different research areas such as communication technologies, biology, chemistry, power converters, economics, where chaotic systems are proven to be very useful [1-6]. Over the last decades until recently, several interesting chaotic systems with a lot of potential applications, such as the Rössler system,the Chen system, the Duffing forced oscillation system, the Lü-Chen system, the Vaidyanathan systems, etc., have been introduced [2,7-12].

In various applications of chaotic systems, the possibility of controlling or ordering chaotic systems is very important for many practical reasons. For instance, in some cases, chaotic, messy, irregular, or disordered system response with little useful information content is unlikely to be undesirable, while in other cases (e.g. fluid mixing, random number generator, etc.) chaos is the desired system response [11]. Therefore, the process of chaos control can be understood as a transition between chaos and order and, sometimes, from chaos to chaos (synchronization), depending on the application of interest [13, 14].

Chaotic systems are known to be highly sensitive to parameter changes. In most practical applications, these changes are challenging to avoid. They may be caused by several factors such as the system's operating conditions, the environment, the temperature, just to name a few. Therefore, it is necessary to apply controllers to chaotic systems in order to ensure their good performances despite these perturbations for which the upper bounds are unknown, referred to as mismatched perturbations.

Since the early nineties, the problem of chaos control has attracted attention of researchers and engineers. A particular technique has been introduced, which is widely used to design controllers with no requirement on prior knowledge of the system's parameters. This technique is called adaptive control. Adaptive control can be either direct or indirect. In direct adaptive control, the controller's parameters (the approximation of the nonlinear function related to the unknown parameters) are directly adjusted and no effort is made for identifying the plant parameters, while in indirect adaptive control the plant parameters are estimated and their values are used to adjust the controller [13]. Over the recent decades, many publications have been made where adaptive control of some existing and/or newly introduced chaotic systems have been addressed. In [6], a new two-scroll chaotic system is proposed with its qualitative properties. The authors also designed an indirect adaptive feedback controller, which stabilizes the states of the new system to zero even though the system's parameters are unknown. In [2], two novel chaotic systems, characterized by a hyperbolic sinusoidal (or cosinusoidal) nonlinearity and two quadratic nonlinearities are presented with their qualitative analysis. Their feedback adaptive controllers are devised to bring them to synchronization even though the systems' parameters are unknown. In [14] a new nonlinear controller is proposed for synchronization of the Lü chaotic system. In [15] nonlinear and linear active controllers are designed for synchronization of the chaotic system introduced in [8]. A comparative analysis is performed in order to assess the effectiveness of the two different controllers on the system. One of the conclusions from this analysis is that with the nonlinear controller, the synchronization error converges to the equilibrium point smoothly with a faster rate than with the active controller. In [16], synchronization of the Lorenz system is addressed with a Sliding Mode Control (SMC) approach based on optimal finite time convergent and integral sliding mode surface. The authors considered that perturbation on the system can be subdivided into two parts, which are the unmatched and the matched parts, and then designed a controller with regards to each of these parts.

Compared to available published works, the contribution of this paper can be summarized as follows:

(a) Introduction of a new chaotic system, which can lead to multiple potential applications, for instance in telecommunication systems, laser technology, chemistry, etc.
(b) Design of an Indirect Robust Adaptive Sliding Mode Controller IRASMC for controlling the new chaotic

system. The designed controller can be used either for synchronizing the system with another different chaotic system, or for suppressing its chaotic behavior by forcing the system's output to track a non-chaotic trajectory. No discontinuous function is used in the control law so that the chattering phenomenon (very high frequency, which can excite some unmodelled dynamics), which is the common drawback of the Sliding Mode Control approach, is avoided. The designed controller doesn't need any prior information on the system's parameters, and shows robustness against mismatched disturbance or unknown system's parameters changes. Another advantage is that it also allows online identification of the system's parameters. One important fact to be mentioned here is that the same controller's design approach used here can be easily applied for the design of controllers for other chaotic systems or nonlinear square Multi Input Multi Output (MIMO) systems with parameters uncertainties.

(c) Application of the design approach available in the literature for MIMO systems often used for chaos synchronization (see e.g. in [2,7,16]), to design another Indirect Adaptive Nonlinear Controller (IANC) for the same system and comparison of its performance with the IRASMC's performances in terms of synchronization error, robustness and system identification ability.

The rest of this paper is organized as follows: section 2 presents the new chaotic system with some of its basic properties; in section 3, the IRASMC is designed for the new chaotic system; in section 4, using one of the traditional approaches for nonlinear controller design, the IANC is developed; section 5 presents the results of MATLAB simulations of the control systems designed in the two previous sections, and section 6 ends this paper with a conclusion.

2. The New Chaotic System and Its Properties

The chaotic system proposed in this paper is described as the following nonlinear autonomous continuous system of differential equations:

$$\begin{cases} \dot{x}(t) = a\big(y(t) - x(t)\big) \\ \dot{y}(t) = -cx(t) + z(t)^4 \\ \dot{z}(t) = bz(t) - x(t)z(t) \end{cases} \qquad (1)$$

where $a, b,$ and c are positive constant parameters of the chaotic system, and $x(t), y(t)$ and $z(t)$ are the system's state variables.

Remark 1: For simplicity in notations, all the state variables will simply be written as x, y and z in all the subsequent parts.

System (1) can be rewritten in the vector form as:

$$\dot{\boldsymbol{X}} = \boldsymbol{F}(\boldsymbol{X}) \qquad (2)$$

where $\boldsymbol{X}^{\boldsymbol{T}} = [x, y, z]$ and $\boldsymbol{F}(\boldsymbol{X}) = [f_1(\boldsymbol{X}),\ f_2(\boldsymbol{X}), f_3(\boldsymbol{X})]^T$ with $f_1(\boldsymbol{X}) = a(y - x)$, $f_2(\boldsymbol{X}) = -cx + z^4$ and $f_3(\boldsymbol{X}) = bz - xz$.

Whenparameters are chosen as $a = 1.8$, $b = 3$ and $c = 10$, system (1) undergoes chaotic behavior. This can be observed in Fig. 1. This figure shows results of a MATLAB simulation of system (1) with the previously mentioned parameter values when initial condition are chosen as$(0.1, 0.8, 1.2)$.

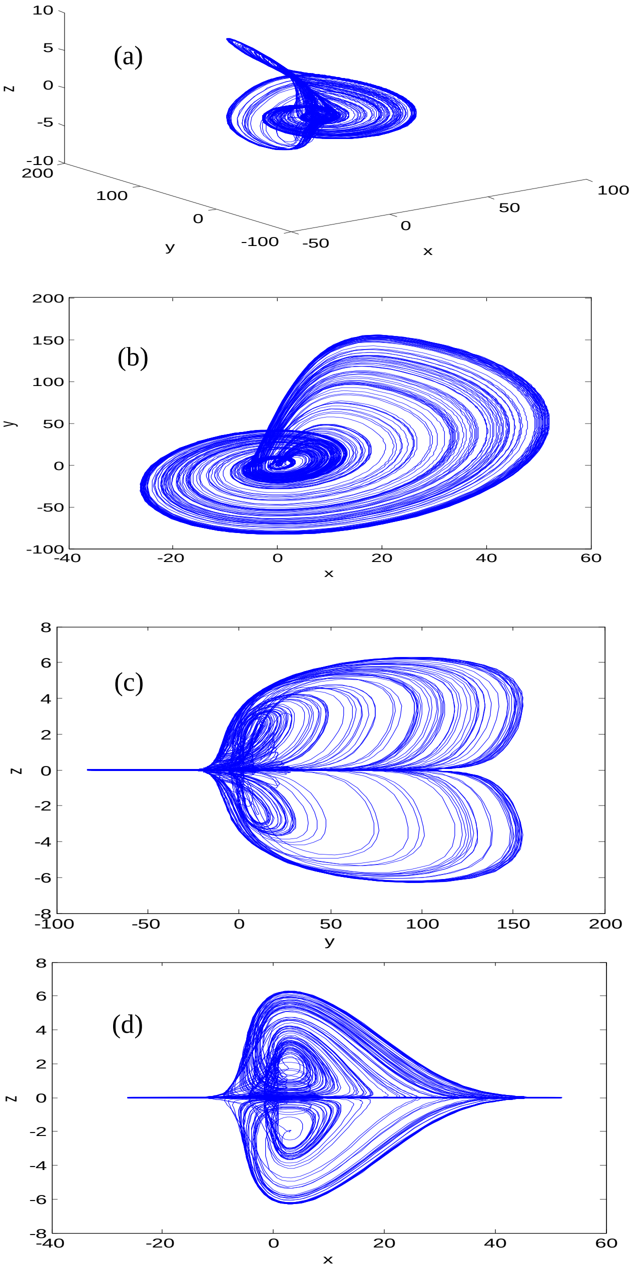

Fig. 1. (a) 3D view of the state variables x, y and z; (b) (x, y) phase portait; (c) (y, z) phase portrait; (d) (x, z) phase portrait

2.1 System's equilibrium points

The equilibrium points are found by solving the equation $\boldsymbol{F}(\boldsymbol{X}) = \boldsymbol{0}$to obtain:

$$\begin{cases} x = b \\ y = b \\ z = \pm(cb)^{\frac{1}{4}} \end{cases} \qquad (3)$$

The system's real equilibrium points are: $E_1(0, 0,0)$, $E_2\left(3,3, \sqrt[4]{30}\right)$ and $E_3\left(3,3, -\sqrt[4]{30}\right)$.
The Jacobian matrix of Eq. (2)is:

$$J(\boldsymbol{X}) = \begin{bmatrix} \frac{\partial f_1(X)}{\partial x} & \frac{\partial f_1(X)}{\partial y} & \frac{\partial f_1(X)}{\partial z} \\ \frac{\partial f_2(X)}{\partial x} & \frac{\partial f_2(X)}{\partial y} & \frac{\partial f_2(X)}{\partial z} \\ \frac{\partial f_3(X)}{\partial x} & \frac{\partial f_3(X)}{\partial y} & \frac{\partial f_3(X)}{\partial z} \end{bmatrix} = \begin{bmatrix} -a & a & 0 \\ -c & 0 & 4z^3 \\ -z & 0 & b-x \end{bmatrix} (4)$$

For the equilibrium point $E_1(0,0,0)$ we have:

$$J(\boldsymbol{E_1}) = \begin{bmatrix} -1.8 & 1.8 & 0 \\ -10 & 0 & 0 \\ 0 & 0 & 3 \end{bmatrix} (5)$$

To find the Eigen value, let's solve the characteristic equation $det[\lambda I - J(\boldsymbol{E_1})] = 0$, where I is a 3×3 identity matrix. We obtain $\lambda_1 = 3, \lambda_2 = -5.9 + j9.12$ and $\lambda_3 = -5.9 - j9.12$. As at this point one of the Eigen values has a positive real part while the others have negative real parts, the equilibrium point E_1 is a saddle point. Hence this equilibrium point is unstable.

Using (4) for the equilibrium points $E_2(3,3,2.3403)$ and $E_3(3,3,-2.3403)$to get the Jacobian matrix, and solving the corresponding characteristic equation, we obtain the Eigen values as: $\lambda_1 = -11.89, \lambda_2 = 0.04 + j10.91$ and $\lambda_3 = 0.04 - j10.91$. As only one of these Eigen values has a negative real part, the equilibrium points $E_2(3,3,2.3403)$ and $E_3(3,3,-2.3403)$ areunstable node for system (1). Hence, this system has no stable equilibrium points.

2.2 Lyapunov Exponents and Lyapunov dimension

In order to measure the exponential rates of divergence or convergence of nearby trajectories in the phase space, we need to find the Lyapunov exponents. These Lyapunov exponents are also a quantitative measure of the system's sensitive dependence on the initial conditions. The system has multiple Lyapunov exponents; their number is equal to the dimension of the phase space. If one speaks about the Lyapunov exponent, the largest one is meant. The mean growth rate of the distance $\|\delta x(t)\|/\|\delta x_0\|$ between neighbouring trajectories is given by the largest Lyapunov exponent, which can be estimated for long (but not too long) time t as [17]:

$$\lambda \cong \frac{1}{t} \ln \frac{\|\delta x(t)\|}{\|\delta x_0\|} \qquad (6a)$$

Using the algorithm presented in [18] with the time series data obtained in MATLAB for the system simulated with the initial condition [0.1 0.8 1.2] and the aforementioned set of parameters, we obtain three Lyapunov exponents as: $L_1 = 2.9989, L_2 = -0.9$ and $L_3 = -0.8989$. These results are depicted in Fig. 2, which shows the dynamics of the Lyapunov exponents. The Largest Lyapunov exponent of the system is 2.9977. It is known that any dissipative dynamical system must have at least one negative exponent [18]. As in this case there are two negative exponents, then system (1) is a dissipative system. The fact that we have at least one positive Lyapunov exponent is evidence that the attractor for this dissipative system is "chaotic". The corresponding Kaplan-Yorke Lyapunov dimension is calculated as follows [2]:

$$D_L = 2 + \frac{L_1 + L_2}{|L_3|} = 4.3373 (6b)$$

This value of the Lyapunov dimension also provides information on the sensitivity of system (1) to changes in parameters and initial condition. The higher this value is, the higher is the sensitivity level.

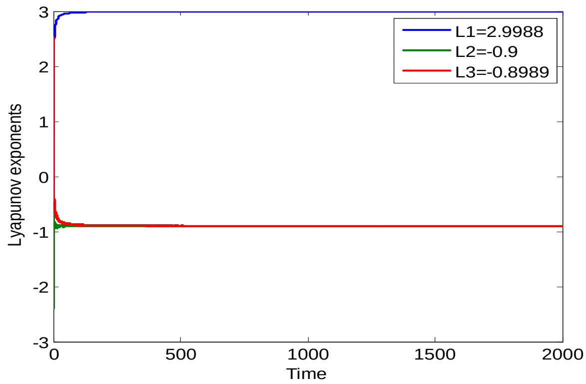

Fig. 2. Dynamics of the Lyapunov exponents

3. Indirect Robust Adaptive Sliding Mode Chaos Controller (IRASMC) design

3.1 Problem statement

We consider the new choatic system as a square MIMO system given by the equations:

$$\begin{cases} \dot{x} = a(y-x) + u_1(t) \\ \dot{y} = -cx + z^4 + u_2(t) (7) \\ \dot{z} = bz - xz + u_3(t) \end{cases}$$

where a, b and c are uncertain parameters related to the first, the second and the third equation, respectively;$u_1(t)$, $u_2(t)$ and $u_3(t)$ are the three input or control signals forthe three subsystems corresponding to state variables x, y and z, which are the system's outputs.

Assumption 1: All the states of system (7) are available through measurement.

The goal is to design the controller $\boldsymbol{u} = [u_1(t), u_2(t), u_3(t)]^T$ such that the outputs x, y and z are forced to track the desired trajectories x_d, y_d and z_d, respectively, dispite the unknown system's parameters.

Let us denote $e_1 = x - x_d$, $e_2 = y - y_d$ and $e_3 = z - z_d$ the tracking errors for the three ouputs. The control objective will be met only if $\lim_{t\to\infty} e_1 = 0$, $\lim_{t\to\infty} e_2 = 0$ and $\lim_{t\to\infty} e_3 = 0$. While making sure this control objective is met, another problem that will be simultaneously addressed is the identification of the system's parameters.

3.2 Controller design

In this subsection we present the design procedure for controller signals$u_1(t), u_2(t)$ and $u_3(t)$ such that the system stability is guaranteed regardless of the changes in the system's parameters, which are to be identified.

Let us select the sliding variable, which gives the error dynamics, as follows:

$$\boldsymbol{s}(t) = \begin{bmatrix} s_1(t) \\ s_2(t) \\ s_3(t) \end{bmatrix} = \begin{bmatrix} \lambda_1 & 0 & 0 \\ 0 & \lambda_2 & 0 \\ 0 & 0 & \lambda_3 \end{bmatrix} \cdot \begin{bmatrix} e_1(t) \\ e_2(t) \\ e_3(t) \end{bmatrix}$$

(8)

where λ_1, λ_2, and λ_3 are positive design parameters.

Let's find the time derivative of the first component of vector $\boldsymbol{s}(t)$ as follows:

$$\dot{s}_1(t) = \lambda_1 \dot{e}_1(t) = \lambda_1 ay - \lambda_1 ax + \lambda_1 u_1 - \lambda_1 \dot{x}_d \quad (9)$$

If parameter a is known, we can use the approach based on the reaching law to design a sliding mode controller [19]. Let us select a constant rate reaching given by the expression

$\dot{s}_1(t) = -\lambda_1 \eta s_1(t)$. Equalizingthis late expression with Eq. (9) we derive the first control law as:

$$u_1(t) = -a(y - x) + \dot{x}_d - \eta s_1(t) \quad (10)$$

where $\eta > 0$ is the constant rate.

As parameter a is assumed to be unknown for system (7), the control law given by Eq. (10) cannot be implemented. Therefore we select the controller as follows:

$$u_1(t) = -\hat{a}(t)(y - x) + \dot{x}_d - \eta s_1(t) \quad (11)$$

where $\hat{a}(t)$ is the estimate value of parameter a.

Applying the controller given by Eq. (11) in Eq. (9) we obtain:

$$\dot{s}_1(t) = \lambda_1 (y - x)\left(a - \hat{a}(t)\right) - \eta \lambda_1 s_1 \quad (12)$$

Let us denote $\tilde{a}(t) = a - \hat{a}(t)$ the error on parameter a approximation. Therefore Eq. (12) can be rewritten as:

$$\dot{s}_1(t) = \lambda_1 (y - x)\tilde{a}(t) - \eta \lambda_1 s_1 \quad (13)$$

The time derivative of the second component of vector $\boldsymbol{s(t)}$ is given by:

$$\dot{s}_2(t) = \lambda_1 \dot{e}_2(t) = -\lambda_2 cx + \lambda_2 z^4 + \lambda_2 u_2(t) - \lambda_2 \dot{y}_d \quad (14)$$

For this case, let us select a constant rate reaching given by$\dot{s}_2(t) = -\lambda_2 \eta s_2(t)$. Equalizingthis late expression with Eq. (14) we derive the second control law as:

$$u_2(t) = cx - z^4 + \dot{y}_d - \eta s_2 \quad (15)$$

As parameter c is unknown for system (7), the control law given by Eq. (15) cannot be applied. Therefore we select the controller as follows:

$$u_2(t) = \hat{c}(t)x - z^4 + \dot{y}_d - \eta s_2(t) \quad (16)$$

where $\hat{c}(t)$ is the estimate value of parameter c.

Applying the controller given Eq. (16) in Eq. (14) we obtain:

$$\dot{s}_2(t) = -\lambda_2 x\left(c - \hat{c}(t)\right) - \eta \lambda_2 s_2(t) \quad (17)$$

Let's denote $\tilde{c}(t) = c - \hat{c}(t)$ the error on parameter c approximation. Therefore Eq. (17) can be rewritten as:

$$\dot{s}_2(t) = -\lambda_2 x\tilde{c}(t) - \eta \lambda_2 s_2 \quad (18)$$

The time derivative of the third component of vector $s(t)$ is found as follows:

$$\dot{s}_3(t) = \lambda_1 \dot{e}_3(t) = \lambda_3 bz - \lambda_3 xz + \lambda_3 u_3 - \lambda_3 \dot{z}_d \quad (19)$$

For this case, let us select a constant rate reaching law given by$\dot{s}_3(t) = -\lambda_3 \eta s_3(t)$. Equalizingthis late expression with Eq. (19), if parameter b is known we derive the first control law as:

$$u_3(t) = -bz + xz + \dot{z}_d - \eta s_3 \quad (20)$$

As parameter b is unknown for system (7), the control law expressed by Eq. (20) cannot be applied. Therefore, we select the controller as follows:

$$u_3(t) = -\hat{b}(t)z + xz + \dot{z}_d - \eta s_3(t) \quad (21)$$

where $\hat{b}(t)$ is the estimate value of parameter b.

Applying controller (21) in (19) we obtain:

$$\dot{s}_3(t) = \lambda_3 bz - \lambda_3 \hat{b}z - \eta \lambda_3 s_3(t) \quad (22)$$

Let's denote $\tilde{b}(t) = b - \hat{b}(t)$ the error on parameter b approximation. Therefore (22) can be rewritten as:

$$\dot{s}_3(t) = \lambda_3 z\tilde{b}(t) - \eta \lambda_3 s_3(t) \quad (23)$$

In order to select the parameter estimation update rules and to prove that applying controllers given by Eqs. (11), (16) and (21) the system stability is guaranteed, and the control objective is met in finite time, let's selected the definite positive Lyapunov function as:

$$V = \frac{1}{2}\left(s_1^2 + s_2^2 + s_3^2 + \tilde{a}^2 + \tilde{b}^2 + \tilde{c}^2\right) \quad (24)$$

where the independent variable (t) is avoided for simplicity in notations, and check if $\dot{V}(t) \le 0$ for all t.

Deriving the Lyapunov function (24) with respect to time t, and applying (13), (18), (23),$\dot{\tilde{a}} = -\dot{\hat{a}}$, $\dot{\tilde{b}} = -\dot{\hat{b}}$ and $\dot{\tilde{c}} = -\dot{\hat{c}}$, we obtain:

$$\begin{aligned}\dot{V} &= s_1\dot{s}_1 + s_2\dot{s}_2 + s_3\dot{s}_3 + \tilde{a}\dot{\tilde{a}} + \tilde{b}\dot{\tilde{b}} + \tilde{c}\dot{\tilde{c}} \\ &= s_1\lambda_1(y - x)\tilde{a} - \eta\lambda_1 s_1^2 - s_2\lambda_2 x\tilde{c} \\ &\quad + s_3\lambda_3 z\tilde{b} - \eta\lambda_3 s_3^2 - \tilde{a}\dot{\hat{a}} - \tilde{b}\dot{\hat{b}} - \tilde{c}\dot{\hat{c}}\end{aligned}$$

$$= \tilde{a}\left[s_1\lambda_1(y - x) - \dot{\hat{a}}\right] - \tilde{c}\left(s_2\lambda_2 x + \dot{\hat{c}}\right)$$
$$+\tilde{b}\left(s_3\lambda_3 z - \dot{\hat{b}}\right) - \eta\lambda_1 s_1^2 - \eta\lambda_2 s_2^2 - \eta\lambda_3 s_3^2 \quad (25)$$

By setting at zero each of the three first terms of (25) (so that the system's stability will not affected by the parameters' estimation errors), we derive the update rules for the estimates parameters $\hat{a}, \hat{b}$ and $\hat{c}$ as follows:

$$\dot{\hat{a}} = s_1\lambda_1(y - x) \quad (26)$$
$$\dot{\hat{b}} = s_3\lambda_3 z \quad (27)$$
$$\dot{\hat{c}} = -s_2\lambda_2 x \quad (28)$$

Applying the update rules (26), (27) and (28) in (25) we obtain:

$$\dot{V} = -\eta\lambda_1 s_1^2 - \eta\lambda_2 s_2^2 - \eta\lambda_3 s_3^2 \quad (29)$$

As $\eta, \lambda_1, \lambda_2$ and λ_3 are positive constant design parameters, $\dot{V} \le 0$, therefore the system stability is guaranteed despite changes in the system's parameters, and $\lim_{t\to\infty} e_1(t) = 0$, $\lim_{t\to\infty} e_2(t) = 0$ and $\lim_{t\to\infty} e_3(t) = 0$. The system's parameters are identified by solving Eqs. (26)-(28).

The functioning principle of the control system is summarized in Fig. 3 where all the components are represented.

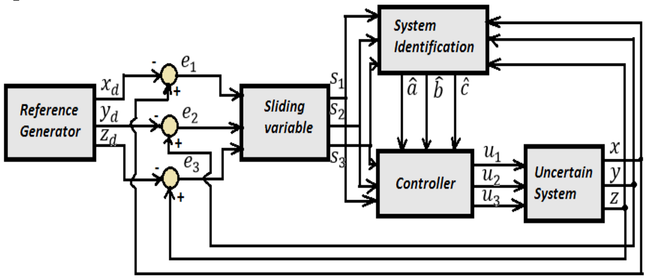

Figure 1: Block diagram of the IRASMC

4. Indirect Adaptive Nonlinear Controller (IANC) design for Chaos synchronization

In this section we design an Indirect Adaptive Nonlinear Controller (IANC) for system (7) using the same approach as in many publications about chaos synchronization (see in [2], [14], [20], for instance).

We consider the master system being the homogenous system (1), rewritten as follows:

$$\begin{cases} \dot{x}_m(t) = a\big(y_m(t) - x_m(t)\big) \\ \dot{y}_m(t) = -cx_m(t) + z_m(t)^4 \quad (30) \\ \dot{z}_m(t) = bz_m(t) - x_m(t)z_m(t) \end{cases}$$

and the slave system being the nonhomogeneous system (7), rewritten as follows:

$$\begin{cases} \dot{x}_s(t) = a\big(y_s(t) - x_s(t)\big) + u_1(t) \\ \dot{y}_s(t) = -cx_s(t) + z_s(t)^4 + u_2(t) \quad (31) \\ \dot{z}_s(t) = bz_s(t) - x_s(t)z_s(t) + u_3(t) \end{cases}$$

Remark 2: In the subsequent development, the independent variable t will be ignored for simplicity in notation.

Let's define the synchronization errors as follows:

$e_1 = x_s - x_m$ (32)
$e_2 = y_s - y_m$ (33)
$e_3 = z_s - z_m$ (34)

In order to find the expression for the synchronization errors dynamics, let's use the time derivatives of (32), (33) and (34), and apply (30) and (31) as follows:

$$\begin{cases} \dot{e}_1 = \dot{x}_s - \dot{x}_m = a(y_s - y_m) - a(x_s - x_m) + u_1 \\ \dot{e}_2 = \dot{y}_s - \dot{y}_m = -c(x_s - x_m) + z_s^4 - z_m^4 + u_2 \quad (35) \\ \dot{e}_3 = \dot{z}_s - \dot{z}_m = b(z_s - z_m) - x_s z_s + x_m z_m + u_3 \end{cases}$$

Using (32), (33) and (34) in (35) we obtain:

$$\begin{cases} \dot{e}_1 = a(e_2 - e_1) + u_1 \\ \dot{e}_2 = -ce_1 + e_3(z_s + z_m)(z_s^2 + z_m^2) + u_2 (36) \\ \dot{e}_3 = be_3 - x_s z_s + x_m z_m + u_3 \end{cases}$$

As parameters a, b and c are unknown, using (36) equalized to zero, we can design the adaptive nonlinear controllers with the estimates parameters$\hat{a}$, $\hat{b}$ and $\hat{c}$ as follows:

$u_1 = -\hat{a}(e_2 - e_1) - \lambda_1 e_1$ (37)
$u_2 = \hat{c}e_1 - e_3(z_s + z_m)(z_s^2 + z_m^2) - \lambda_2 e_2$ (38)
$u_3 = -\hat{b}e_3 + x_s z_s - x_m z_m - \lambda_3 e_3$ (39)

whereλ_1, λ_2 and λ_3 are positive design paramters correponding to the rate of exponential convergence of slave system's state to the trajectories of the master system's states.

Applying (37), (38) and (39) into (36) we obtain:

$$\begin{cases} \dot{e}_1 = (a - \hat{a})(e_2 - e_1) - \lambda_1 e_1 \\ \dot{e}_2 = -(c - \hat{c})e_1 - \lambda_2 e_2 \quad (40) \\ \dot{e}_3 = \big(b - \hat{b}\big)e_3 - \lambda_3 e_3 \end{cases}$$

Let's denote $e_a = a - \hat{a}$, $e_b = b - \hat{b}$ and $e_c = c - \hat{c}$ the parameter estimation errors and apply them in (40). We obtain:

$$\begin{cases} \dot{e}_1 = e_a(e_2 - e_1) - \lambda_1 e_1 \\ \dot{e}_2 = -e_c e_1 - \lambda_2 e_2 \quad (41) \\ \dot{e}_3 = e_b e_3 - \lambda_3 e_3 \end{cases}$$

In order to find the parameter estimates' update rules and analyze the system's stability if controllers (37), (38) and (39) are applied, we select a positive definite Lyapunov function as follows:

$$V = \frac{1}{2}(e_1^2 + e_2^2 + e_3^2 + e_a^2 + e_b^2 + e_c^2) \quad (42)$$

and check if $\dot{V}(t) \le 0$ for all t.

Using the time derivative of (42), applying (41) and $\dot{e}_a = -\dot{\hat{a}}$, $\dot{e}_b = -\dot{\hat{b}}$ and $\dot{e}_c = -\dot{\hat{c}}$ we obtain:

$$\dot{V} = e_1\dot{e}_1 + e_2\dot{e}_2 + e_3\dot{e}_3 + e_a\dot{e}_a + e_b\dot{e}_b + e_c\dot{e}_c$$

$$\begin{aligned} \dot{V} = e_1 \ [e_a(e_2 - e_1) - \lambda_1 e_1] + e_2(-e_c e_1 - \lambda_2 e_2) \\ + e_3(e_b e_3 - \lambda_3 e_3) - e_a\dot{\hat{a}} - e_b\dot{\hat{b}} - e_c\dot{\hat{c}} \\ = e_a[e_1(e_2 - e_1) - \dot{\hat{a}}] \ + e_b\left(e_3^2 - \dot{\hat{b}}\right) - e_c(e_1 e_2 + \dot{\hat{c}}) \\ -\lambda_1 e_1^2 - \lambda_2 e_2^2 - \lambda_3 e_3^2 \end{aligned}$$

(43)

By setting to zero each of the three first terms of (43), we derive the update rules as follows:

$\dot{\hat{a}} = e_1(e_2 - e_1)$ (44)
$\dot{\hat{b}} = e_3^2$ (45)
$\dot{\hat{c}} = -e_1 e_2$ (46)

Applying (44), (45) and (46) in (47) we get:

$$\dot{V} = -\lambda_1 e_1^2 - \lambda_2 e_2^2 - \lambda_3 e_3^2 \le 0 \quad (47)$$

Therefore one can conclude that applying controllers (37), (38) and (39), and using the update rules (44), (45) and (46), the system's stability and exponential convergence towards zero of synchronization errors are guaranteed.

Remark 3: The design used for the IRASMC has the advantage that it allows the controller to be used to track any chaotic or non-chaotic trajectory, while this is not the case with the IANC designed in this section.

5. Simulation

We consider (7) as the slave system first controlled by the IRASMC designed in section 3, and then controlled by the IANC designed in section 4. For the IRASMC the control laws $u_1(t)$, $u_2(t)$ and $u_3(t)$ are given by (11), (16) and (21), respectively. For the IANC the control laws $u_1(t)$, $u_2(t)$

International Journal of Science and Research (IJSR)
ISSN: 2319-7064
ResearchGate Impact Factor (2018): 0.28 | SJIF (2018): 7.426

and $u_3(t)$ are given by (37), (38) and (39). For the two controllers, the design parameters are selected as $\lambda_1 = 1, \lambda_2 = 1, \lambda_3 = 1$ (from a trial and error process); $\eta = 6$ for the IRASMC.

Using the MATLAB solver for Ordinary Differential Equations (ODEs) ode45, with the integration step size selected as $dt = 0.01$, simulation is performed over a period from 0 to 50. During simulation, the controllers are not activated until the simulation time 15. The slave system is considered initially having nominal values for its parameters as $a = 1.8$, $b = 3$ and $c = 10$. The initial state of this system is set as $[10, -1.6, -1.2]$. The initial values of the parameter estimates are selected randomly as $\hat{a} = 3\hat{b} = 1\hat{c} = 4$. In order to test the robustness of the control system, in case of slave system's parameters changes, we assume that, for a given reason, at simulation time $t = 30$ the values of the system's parameters are increased by 25%. Therefore we have:

$$a = \begin{cases} 1.8 & if\ t < 30 \\ 2.25 & elsewhere \end{cases}$$

$$b = \begin{cases} 3 & if\ t < 30 \\ 3.75 & elsewhere \end{cases}$$

$$c = \begin{cases} 10 & if\ t < 30 \\ 12.5 & elsewhere \end{cases}$$

In order to prove the effectiveness of the IRASMC, we perform simulation for two different cases.

Case 1: The control objective is complete synchronization of the slave system with the autonomous system (1) (master). The initial state of the master system (1) is selected as$[1, 0.8, 1.2]$.

Fig. 4 and Fig. 5 show the results of simulation when the slave system is controlled by the IRASMC and by the IANC, respectively. In both figures, one can see that starting from different initial conditions, the states of the master and slave systems evolve on different trajectories before activation of the controllers. At simulation time 15 when the controllers are activated, the states of the slave system enter in complete synchronization with the states of the master system. From the simulation time 30 when the values of the slave system's parameters are increased by 25%, the system controlled by the IRASMC keeps the synchronization error very close to zero (see Fig. 4 (d)) despite the disturbance. This is the evidence of the robustness of the control system in this case. In contrast, as it can be observed in Fig. 5 (d) the synchronization errors increase when the disturbance occurs in the system controlled by the IANC. Another benefit of using the IRASMC is that it allows online system identification. In fact, as shown on Fig. 4 (e), good approximations of the slave system's parameters are obtained as $\hat{a} = 1.8\hat{b} = 2.9325\hat{c} = 10.002$ measured at $t = 25$, and $\hat{a} = 2.2409\hat{b} = 3.7531\hat{c} = 12.5568$ measured at $t = 50$.

In Fig. 5 (e) we can see that with the IANC the approximate values for the parameters are not accurate (their values are too different from the ones previously assumed for simulation).

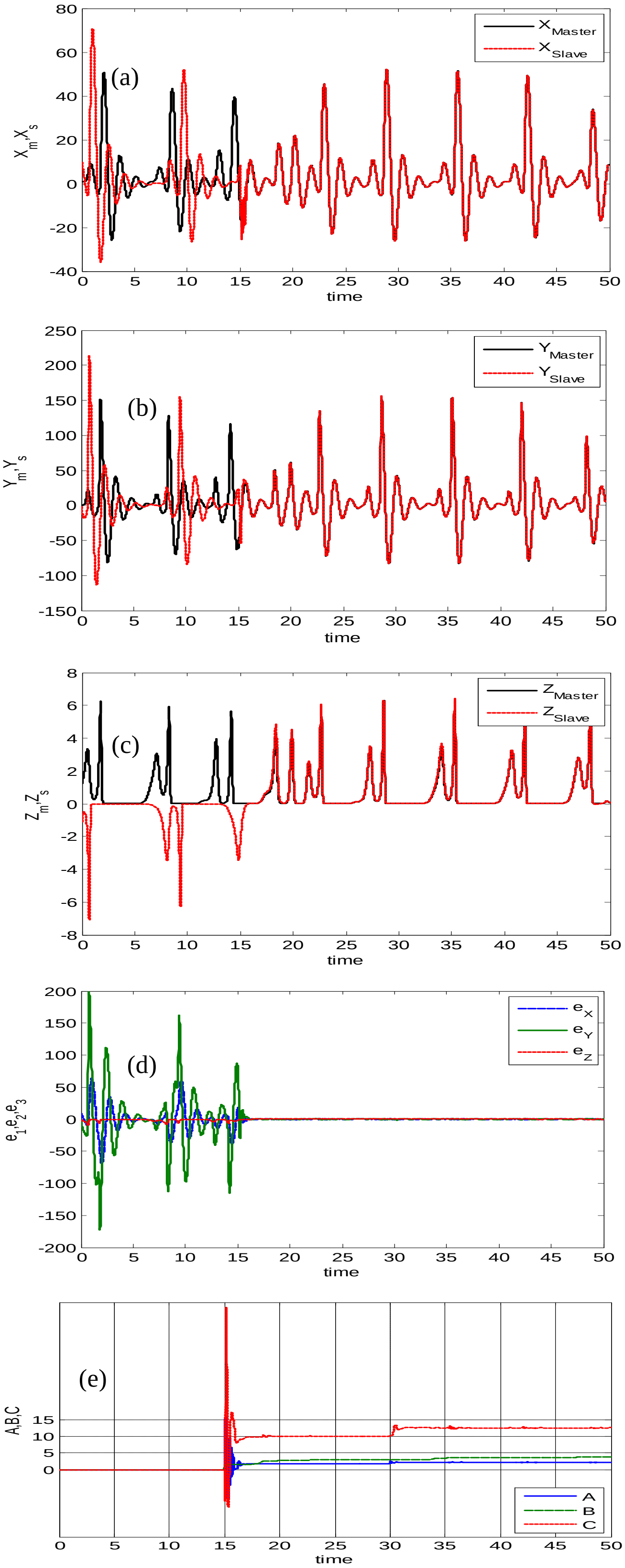

Figure 4. Simulation results when the IRASMC is used for complete synchronization. (a), (b) and (c): State variables of the master and slave systems before and after controller acivation; (d) Synchronization errors on the three state variables; (e) dynamics of the approximate values of paramters.

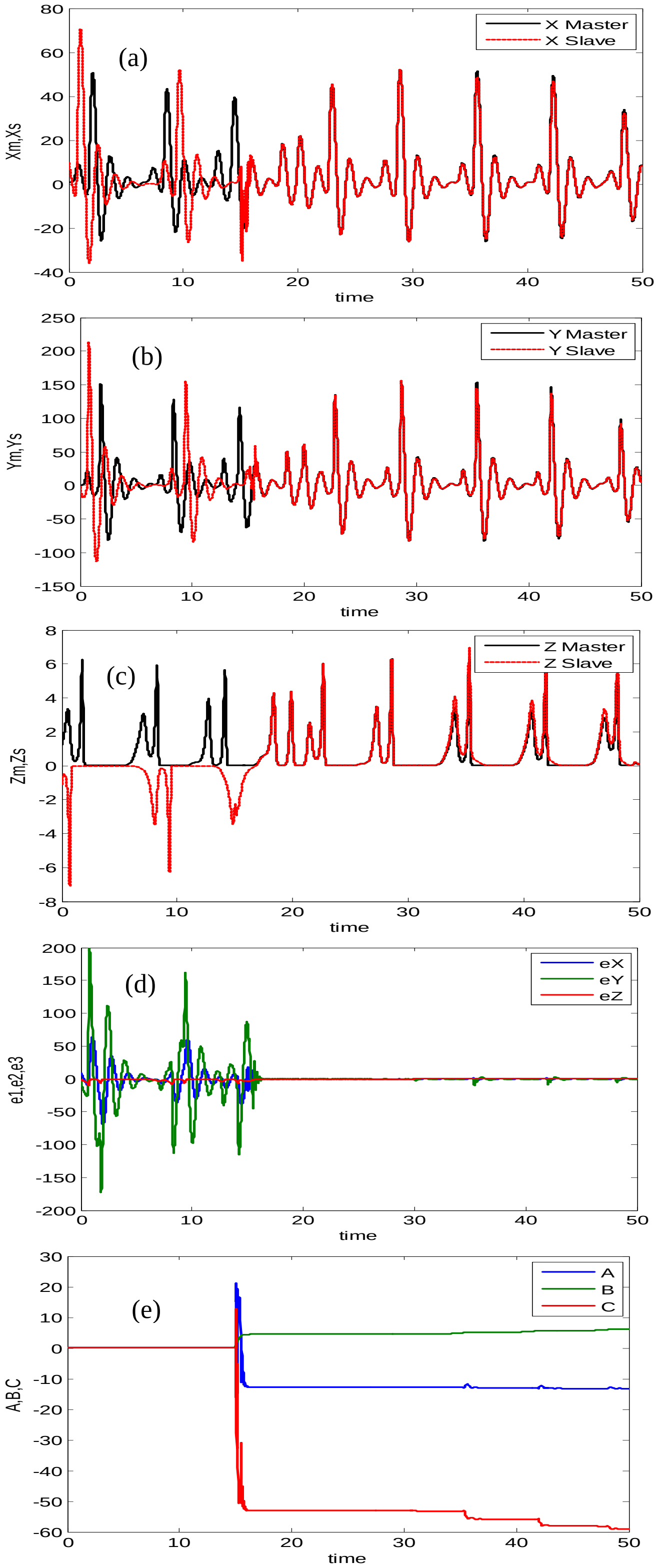

Figure 5. Simulation results when IANC is used for complete synchronization. (a), (b) and (c): State variables of the master and slave systems before and after controller acivation; (d) Synchronization errors on the three state variables; (e) dynamics of the approximate paramters.

Case 2: The control objective is chaos suppression or forcing the system (7) state variables to track a non-chaotic trajectory. For the IRASMC, the design parameters are selected as $\lambda_1 = 5, \lambda_2 = 5$, $\lambda_3 = 5$ and $\eta = 6$ (from a trial and error process).

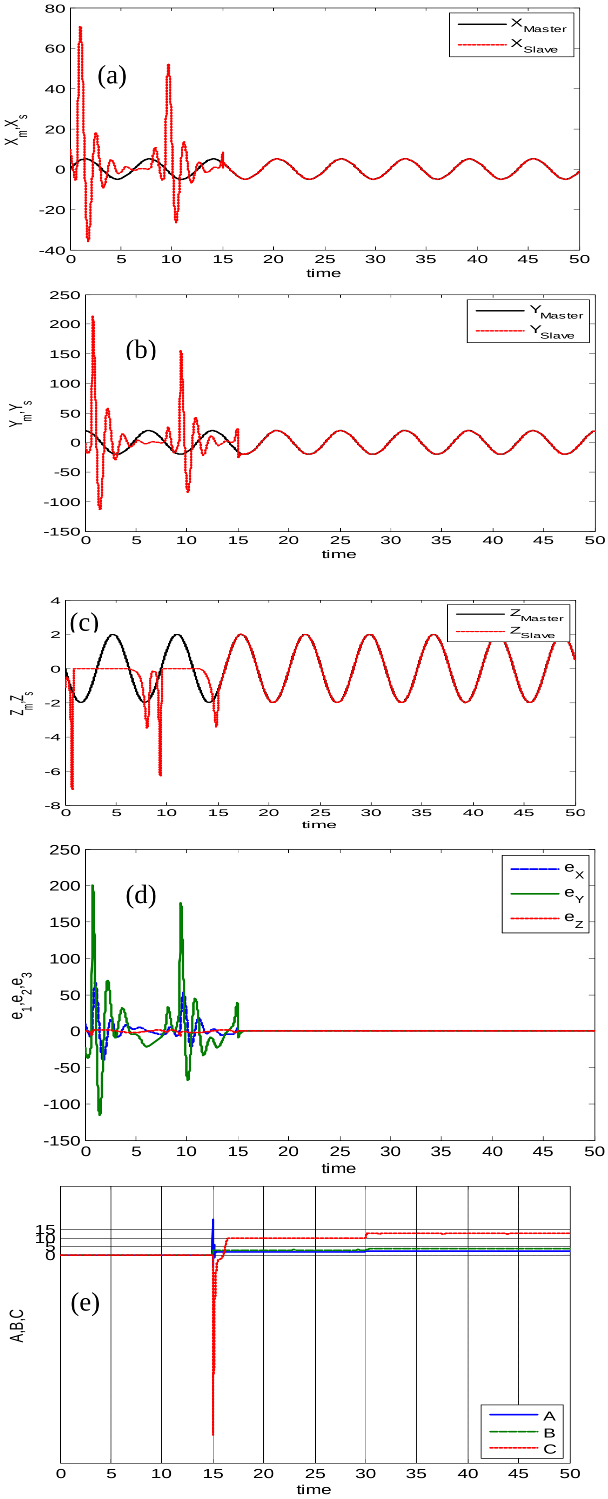

Figure 6: Simulation results when IRASMC is used for chaos suppression. (a), (b) and (c): State variables of the controlled system before and after controller acivation; (d) Tracking errors on the three state variables; (e) dynamics of the approximate paramters.

Simulation is performed with the same initial conditions as in the previous case but with different desired trajectories. The desired trajectories are selected as $x_m = 5\sin(t)$, $y_m = 20\cos(t)$ and $z_m = -2\sin(t)$for the state variable x_s, y_s and z_s, respectively. Fig. 6 shows the simulation results. As one can observe, despite the parameter change or perturbation that occurs at the simulation time 15, the control system tracking errors is not affected.

This is the evidence of the robustness of the IRASMC and its effectiveness in suppressing chaos. As in the previous case, not only the control objective is met, but system identification is also successfully performed. The approximate values for the controlled system as found as $\hat{a} = 1.7988\hat{b} = 2.9641\hat{c} = 9.9324$ measured at $t = 25$, and $\hat{a} = 2.2499$, $\hat{b} = 3.7123$, $\hat{c} = 12.4173$ measured at $t = 50$. The dynamics of these approximations is shown in Fig. 6 (e).

6. Conclusion

A new three dimensional chaotic system is introduced with its basic properties. Assuming that its parameters are unknown, two types of indirect adaptive controllers are devised. Based on the Sliding Mode approach, a new controller is designed. In addition to the robustness property of this controller (the IRASMC) for systems with mismatch disturbances (unknown parameter changes), it also allows system identification whether it is used for complete synchronization or for chaos suppression. Performance it terms of accuracy is also good with the IRASMC. Another Indirect Nonlinear Controller (INC) is designed for the same new system and is proven to not be robust and to not allow accurate system identification.

References

[1] E. N. Lorenz, "Deterministic nonperiodic flow," Journal of the Atmospheric Sciences, vol. 20, pp. 130-141, 1963.
[2] S. Vaidyanathan, "Analysis of Two Novel Chaotic Systems with a Hyperbolic Sinusoidal Nonlinearity and their Adaptive Chaos Synchronization," in Fourth International Conference on Computing, Communications and Networking Technologies (ICCCNT), Tiruchengode, 2013.
[3] B. R. Andrievskii and Fradkov, "Control of Chaos: Methods and Applications," Automation and Remote Control, vol. 65, no. 4, pp. 505-533, 2004.
[4] D. Guegan, "Chaos in Economics and Finance," Annual Rev. Control, vol. 33, no. 1, pp. 89-93, 2009.
[5] M. S. Baptista, E. E. Macau and C. Grebogi, "Integrated chaos- based communication," Acta Astron, vol. 54, pp. 153-157, 2004.
[6] S. Vaidyanathan and Madhavan, "Adaptive Control of a Two-Scroll Novel Chaotic System with a Quadratic Nonlinearity," in International Conference on Science, Engineering and Management Research (ICSEMR 2014), Chennai, 2014.
[7] O. E. Rössler, "An equation for continuous chaos," Physics Letters A, vol. 57, pp. 397-398, 1976.
[8] G. Chen and T. Ueta, "Yet another chaotic attractor," International Journal of Bifurcation, vol. 9, no. 7, pp. 1465-1466, 1999.
[9] J. H. Pérez, M. Figueros, S. A. Rodriguez, and A. Lopez, "Synchronization of chaotic Akgul system by means of feedback linearization and pole placement", IEEE Latin America Transactions, vol. 15, no. 2, pp. 249-256, 2017.
[10] E. E. Mahmoud and F. S. Abood, "A general formula of complex synchronizations with complex scaling factor diagonal matrix and time lag ", Results in Physics, vol. 12, pp. 603-614, 2019.
[11] G. Chen, "Control and anticontrol of chaos," in 1997 1st International Conference on Control of Oscillations and Chaos, St. Petersburg, 1997.
[12] B. R. Andrievskii and A. L. Fradkov, "Control of Chaos: Methods and Applications," Automation and Remote Control, vol. 64, no. 5, pp. 673-713, 2003.
[13] M. Hojati and S. Gazor, "Hybrid Adaptive Fuzzy Identification and Control of Nonlinear Systems," IEEE Transactions of Fuzzy Systems, vol. 10, no. 2, pp. 198-210, 2002.
[14] J. h. Park, "Chaos synchronization of a chaotic system via nonlinear control," Chaos, Solitons and Fractals, vol. 25, pp. 579-584, 2005.
[15] A. B. Saaban, A. B. Ibrahim, M. Shahzad and I. Ahmad, "Identical Synchronization of a New Chaotic System via NonlinearControl and Linear Active Control Techniques: A Comparative Analysis," International Journal of Hybrid Information Technology , vol. 7, no. 1, pp. 211-224, 2014.
[16] X. Guowei, W. Zhenkai and L. Chunqing, "Synchronization of Lorenz System Based on Fast Stabilization Sliding Mode Control," Mathematical Problems in Engineering, vol. 2014, p. 7, 2014.
[17] P. Cvitanovi, R. Artuso, G. Mainieri, G. Tanner and G. Vattay, Chaos: Classical and Quantum, Copenhagen: Niels Bohr Institute, 2012.
[18] A. Wolf, J. B. Swift, H. L. Swinney and J. A. Vastano, "Determining Lyapunov Exponents from a Time Series," Physica D, vol. 16, pp. 285-317, 1985.
[19] J. Liu and X. Wang, Advanced Sliding Mode Control for Mechanical Systems, Berlin: Springer-Verlag, 2011.
[20] S. Vaidyanathan and K. Madhavan, "Adaptive Control of a Two-Scroll Novel Chaotic System with a Quartic Nonlinearity," in International Conference on Science, Engineering and Management Research (ICSEMR 2014), Chennai, 2014.

Author Profile

Baraka Mushage O. has received the Civil Engineer degree in Electrical Engineering from *Université Libre des Pays des Grands Lacs* (ULPGL in Democratic Republic of the Congo), the academic degrees of Diplom-Ingenieur (DI) and Doctor technicae (Dr. techn.) in from the University of Klagenfurt, Austria, in Information Technology.He is currently working at the Department of Electrical and Computer Engineering of the Faculty of Applied Sciences and Technologies of ULPGL, in DRC, as a Researcher and Lecturer. His research interests include nonlinear robust, intelligent and fault tolerant control of dynamical systems.